Studies of Targeting and Intracellular Trafficking of an Anti-Androgen Doxorubicin−Formaldehyde Conjugate in PC-3 Prostate Cancer Cells Bearing Androgen Receptor-GFP Chimera

Peter S. Cogan[‡] and Tad H. Koch[†,‡,*]

Department of Chemistry and Biochemistry, University of Colorado, Boulder, Colorado 80309-0215, and Department of Pharmaceutical Sciences, University of Colorado Health Sciences Center, Denver, Colorado 80262

Received June 18, 2004

The synthesis of a doxorubicin−formaldehyde conjugate bound to the nonsteroidal anti-androgen cyanonilutamide, via a cleavable tether, and binding of the construct to cell free androgen receptor (AR) as a function of tether design were previously reported. Cyanonilutamide bearing a linear alkyne tether bound to the AR better than other designs. Fluorescence microscopy studies of binding of the lead targeted drug, as well as various tethered cyanonilutamides, to the AR and subsequent trafficking of the resulting AR complex in live PC3 prostate cancer cells transfected with AR-green fluorescent protein (GFP) chimera are now described. Cyanonilutamide and cyanonilutamide bonded to a linear alkyne tether caused translocation of AR-GFP to the nucleus. In general, the ability of tethered cyanonilutamides to cause translocation paralleled their binding affinity for the AR. However, a noncleavable form of the lead cyanonilutamide−doxorubicin−formaldehyde conjugate bound to AR-GFP but the resulting complex did not translocate to the nucleus. Binding was apparent from the drugs inhibition of Mibolerone-induced translocation. Direct observation of anthraquinone fluorescence of targeted drug in PC3 cells showed initial cytosolic localization, independent of AR expression, with predominant nuclear localization after sufficient time for release of drug from the targeting moiety. The results indicate that doxorubicin−formaldehyde conjugate bonded to cyanonilutamide via a cleavable linear tether enters PC3 cells, resides in cytosol, binds to the AR if present, and ultimately releases doxorubicin or a doxorubicin derivative to the nucleus.

Introduction

Work in our laboratory, and others, has shown that the concomitant delivery of formaldehyde with doxorubicin, or other anthracyclines, to growing tumor cells leads to a superior antiprolific response relative to the delivery of doxorubicin alone.[1−4] In an attempt to capitalize on this observation, we have recently developed several unique prodrugs of a formaldehyde conjugate of the anthracycline doxorubicin.[1,5,6] We propose that the partial hydrolysis of these prodrugs renders the doxorubicin−formaldehyde Schiff base, which subsequently serves to covalently modify DNA, an event proposed to be more toxic than the mere intercalation of unmodified doxorubicin.[7−10] From among these novel prodrugs we have identified a candidate for development as a tumor targeted source of both doxorubicin and formaldehyde. The N-Mannich base resulting from the condensation of doxorubicin with salicylamide (2-hydroxybenzamide) and formaldehyde, nominally referred to as doxsaliform **1a** (Figure 1), has proven to be a superior cytotoxin relative to the parent drug against both doxorubicin sensitive and resistant cultured human tumor cells.[5]

We are currently studying the feasibility of targeting the N-Mannich base doxsaliform to a variety of tumor specific receptors including estrogen receptor,[11,12] integrin $\alpha_v\beta_3$,[13,14] and aminopeptidase N.[14] These proteins are found to be overexpressed in clinical tumors and

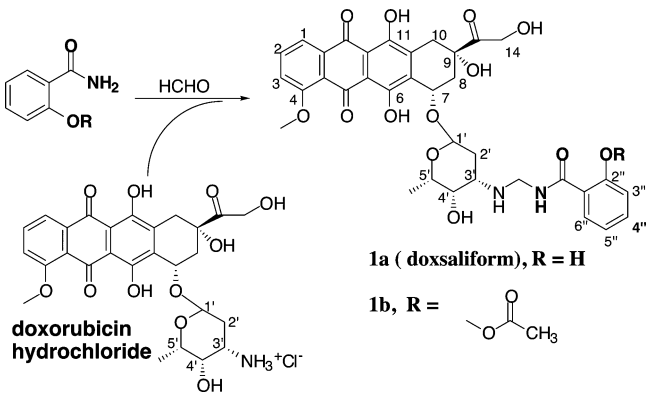

Figure 1. Synthesis of the prodrug doxsaliform in its unprotected (**1a**) and protected (**1b**) forms. Formalin was added to a 55 °C DMF solution of salicylamide 15 min before the addition of doxorubicin hydrochloride.

derivative cell lines, or in the requisite developing tumor vasculature, and are proposed to serve as viable targets for tissue selective drug delivery. We have also recently completed the synthesis of a series of androgen receptor (AR) targeted molecules (Figure 2) for the delivery of the N-Mannich base doxsaliform to prostate-derived neoplasms. Cell free analysis of the competitive binding affinity of this series for the androgen receptor in the presence of the steroidal ligand Mibolerone indicates that several of the tested compounds do indeed bind competitively and specifically to the AR with IC_{50} values ranging from >1.0 μM to 49 nM (Table 1).[15] Although these results are promising, it is necessary to further characterize the binding event in whole cells so as to fully realize the extent of AR-mediated drug delivery.

* Corresponding author. Phone 303-492-6193, fax 303-492-5894, e-mail tad.koch@colorado.edu.
† University of Colorado.
‡ University of Colorado Health Sciences Center.

10.1021/jm0495226 CCC: $27.50
Published on Web 10/02/2004

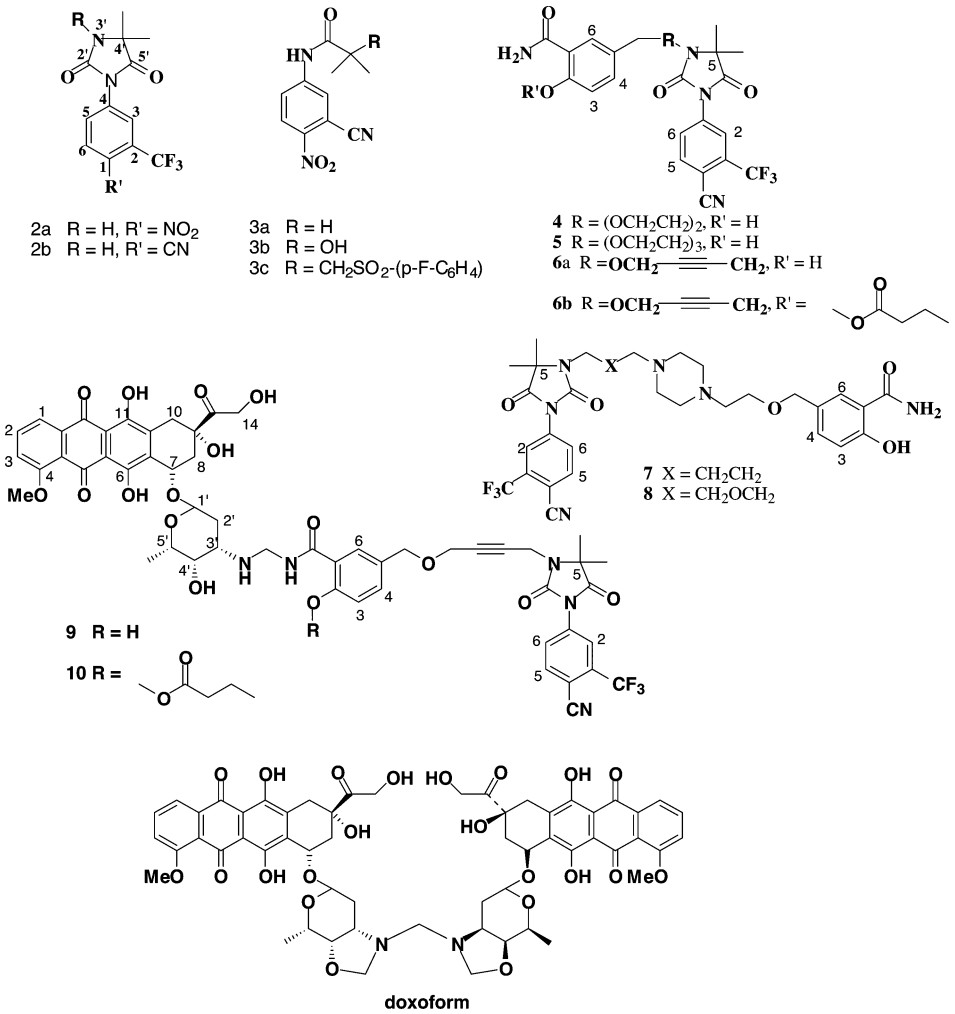

Figure 2. Structures of various nonsteroidal antiandrogens (**2**, **3**), AR targeting molecules (**4**−**10**), and the highly toxic, prodrug, doxorubicin−formaldehyde conjugate, doxoform.

Table 1. IC_{50} and Relative Binding Affinity Values Determined from Competitive Binding for the Human AR of the Various Test Ligands against 1.0 nM ^{3}H-Mibolerone in PC3/AR Cell Lysate at 4 °C[15]

test compound	IC_{50}, nM	RBA
2a	9	100
2b	6	150
4	77	13
5	332	3
6a	49	18
7	>1000	<1
8	346	3
9	90	10
10	63	14
flutamide	154	6
salicylamide	≫1000	≪1

While immunohistochemical staining of various normal tissues indicates only low level expression outside of the reproductive tract,[16] the androgen receptor has been identified in a wide array of human tumors in both male and female patients. Carcinomas of the breast,[17,18] ovary,[19] esophagus,[20] lung,[21] and prostate[22] have all been shown to express the AR at various levels. The expression or overexpression of AR in the majority of human prostate tumors also suggests that it may be required for growth in prostate cancer (CaP).[22,23]

The AR exists primarily as a cytosolic receptor[24] in complex with several heat-shock proteins (hsp70, hsp90, and hsp56−59). Ligand binding leads to dissociation of the heat-shock proteins, homodimerization, and translocation into the nucleus where the dimeric receptor recognizes hormone responsive elements and various components of the transcription machinery.[25,26] The receptor is often overexpressed in hormone refractory prostate cancer and is also known to acquire mutations that lead to promiscuous binding of various nonandrogen ligands.[25,27] Several groups have successfully ligated the cDNA of the androgen receptor to that of a modified green fluorescent protein (GFP) in a construct which encodes the chimeric AR-GFP product.[24,26,28] In the absence of ligand, AR-GFP has been shown to localize in the cytoplasm of transfected cells. However, upon binding of dihydrotestosterone (DHT), or other appropriate agonists, the receptor is observed to translocate into the nucleus. Antagonists, on the other hand, vary in their ability to cause migration of the receptor into the nucleus of treated cells.[29] While some do effect a change in cellular localization of the fluorescent receptor, others serve to prevent the nuclear translocation through inhibition of DHT binding. The easily qualified response to receptor binding has been successfully used to ascertain the effect of various agonists and antagonists on cellular localization of the AR. Herein is described the intracellular response of the AR-GFP receptor in PC3 cells upon exposure to a series of AR targeted derivatives of salicylamide, the amide moiety of the N-Mannich base doxsaliform. Also described is

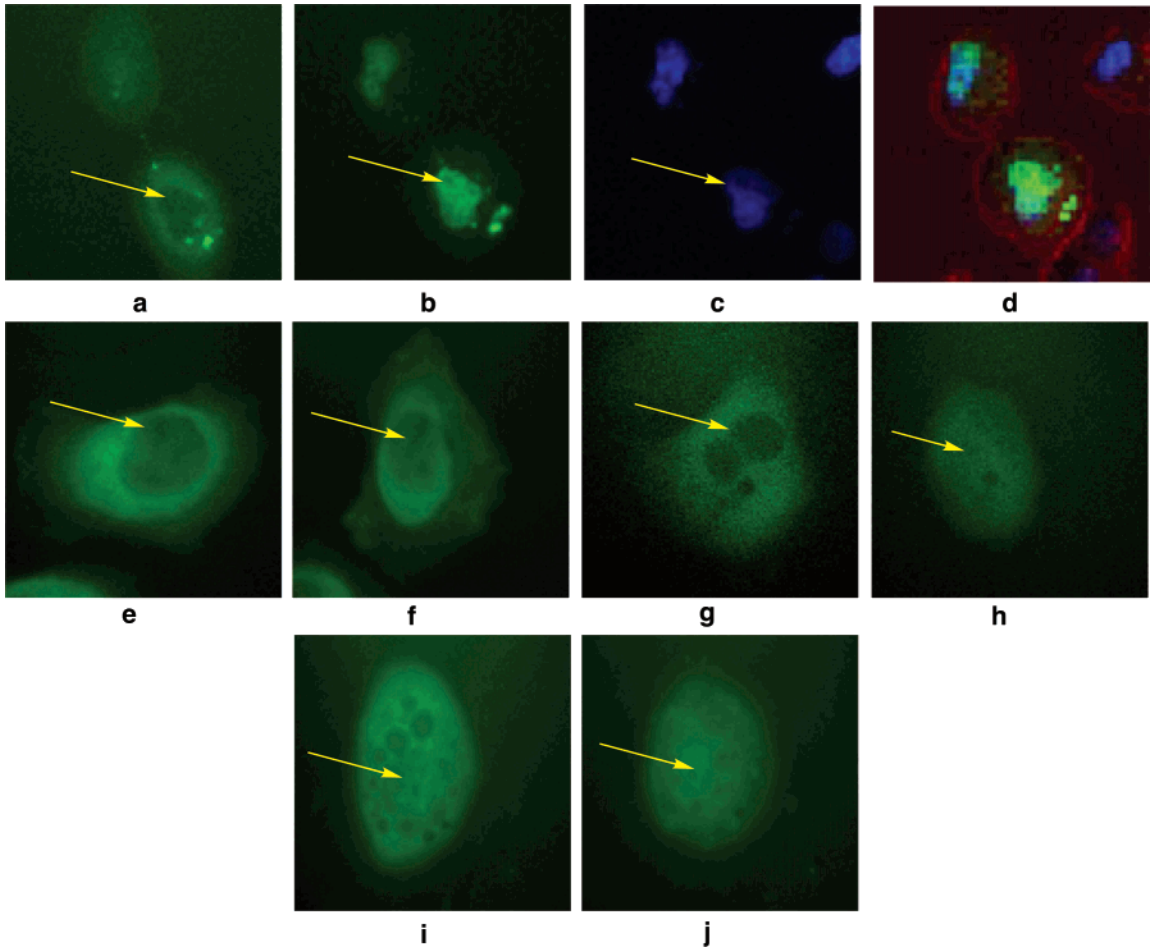

Figure 3. (a) AR-GFP-expressing PC3 cells before and (b) 60 min after treatment with 1.0 nM Mibolerone. Nuclear (yellow arrow) localization of the fluorescent receptor is obvious after 1 h drug treatment; (c) staining pattern of the same cells after fixing and treatment with the nuclear stain DAPI; (d) overlay of b (green), c (blue), and the reflected light micrograph (red) of the fixed cells; (e) cells before and (f) 60 min after treatment with 1.0 μM nilutamide; (g) cells before and (h) 60 min after treatment with 1.0 μM **2b**; (i) cells before and (j) 60 min after treatment with 1.0 μM nilutamide and 1.0 nM Mibolerone.

the action of the doxorubicin N-Mannich base product formed from the most effective targeting compound of the tested series.

Results and Discussion

After establishing that our targeting groups were capable of binding specifically to the AR with reasonable affinity (Table 1),[15] we sought to establish whether the binding event will lead to nuclear delivery of the constructs. PC3 cells were, therefore, grown in six-well plates and transiently transfected with a plasmid containing the AR-GFP construct obtained from Dr. Arun Roy (UTHSC; San Antonio, Texas).[26] After 18 h incubation, the cell culture media was removed and replaced with RPMI 1640 supplemented with 10% fetal bovine serum (FBS) which had been stripped of steroids (and other components) with dextran-coated charcoal.[30] Growth in the stripped media for 18 h allowed for predominantly cytosolic localization of the AR-GFP receptor and also served to remove steroids which can potentially interfere with the binding of the test compounds. The transfected cells were then treated with various targeting groups and controls in the presence or absence of Mibolerone. Mibolerone causes nuclear translocation of the AR-GFP receptor in approximately 30 min at concentrations as low as 1.0 nM. Digital imaging of the cells allows for facile analysis of the activity of the various ligands. While we did not perform a statistical analysis of entire cell populations treated with the various ligands, we did observe population-wide response to the active ligands in agreement with the findings of Roy et al.[25,26] The cells photographed were chosen for picture quality but are representative of the response observed across the treated population.

Figure 3a shows live PC3 cells which express the AR-GFP construct. After 1 h treatment with 1.0 nM Mibolerone, the fluorescence appeared to be almost exclusively nuclear (Figure 3b). Following 1 h drug treatment, the cells were fixed with a 1% glutaraldehyde solution and treated with the nuclear stain DAPI. DAPI fluorescence (Figure 3c) indicated that the focal point of the AR-GFP fluorescence after 1 h Mibolerone treatment was, in fact, the nucleus. Similar 1 h treatment of cells with the various AR targeting groups shown in Figure 2 led to a variety of results. Previous work with this system showed that, while the antiandrogen hydroxyflutamide is capable of inducing nuclear translocation of AR-GFP, nilutamide is largely incapable of causing the reaction (Figure 3e + 3f).[29] The binding of nilutamide to AR-GFP was, however, evidenced by its ability to preclude translocation induced by 1.0 nM Mibolerone (Figure 3i + 3j).

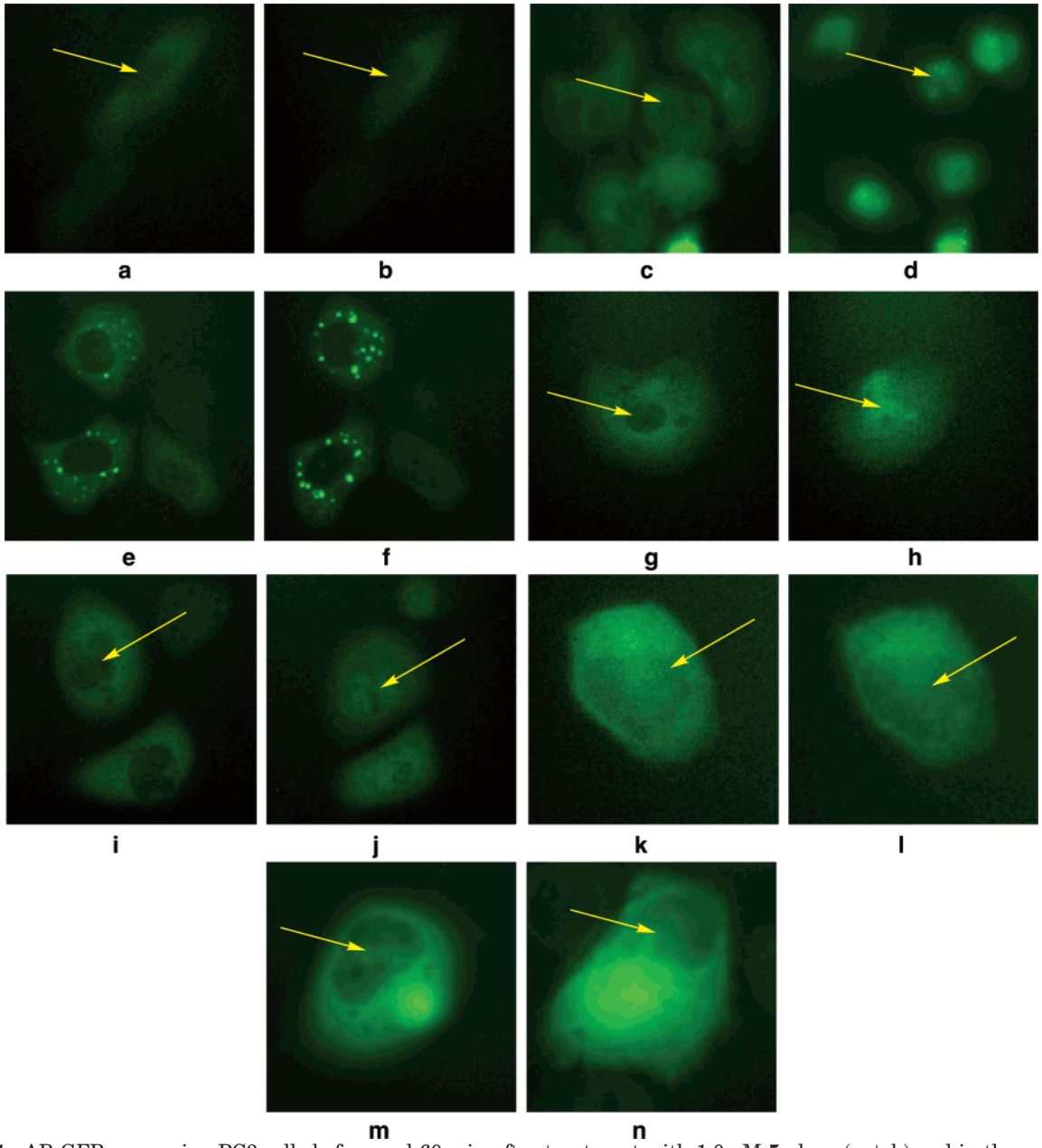

Figure 4. AR-GFP-expressing PC3 cells before and 60 min after treatment with 1.0 μM **5** alone (a + b) and in the presence of 1.0 nM Mibolerone (c + d); 1.0 μM **4** alone (e + f) and in the presence of 1.0 nM Mibolerone (g + h); 1.0 μM **6** (i + j); 1.0 μM **10** alone (k + l) and in the presence of 1.0 nM Mibolerone (m + n).

Compound **2b** was found to bind the AR and, apparently, induce partial translocation as manifest by a clear morphological change and redistribution of fluorescence (Figure 3g + 3h). It must be noted that the effect of **2b** on cells is somewhat ambiguous, as the morphological change and nearly homogeneous distribution of fluorescence could be indicative of simple cytosolic redistribution of AR-GFP leading to nuclear masking. This masking effect, in which a nonfluorescing nucleus would be hidden by excess cytoplasmic GFP in the line of sight, was not observed in any other cells treated with inactive ligands. However, the absence of a clearly discernible nucleus in cells treated with **2b** leaves open this possibility. In any event, it is not clear why the seemingly subtle substitution of the cyano group of **2b** for the nitro moiety of nilutamide leads to a compound that is capable of initiating translocation. Conformational changes induced by ligand binding are known to be required for migration of the AR into the nucleus.[31] The varying activities of structurally similar AR antagonists suggests that antiandrogenic activity is manifested at different stages of AR activation. While hydroxyflutamide **3b** and the structurally similar antiandrogen bicalutamide **3c** do induce the appropriate conformational changes to allow for nuclear translocation and, therefore, must block AR activity at some downstream event, nilutamide apparently acts simply by blocking steroid binding.[29] The structural similarity of the nonsteroidal antiandrogens, however, suggests that small changes to the nilutamide core may be expected to impart the necessary receptor interactions to induce a conformational change that will lead to nuclear localization of the receptor.

Treatment of AR-GFP-expressing cells with the targeting constructs **5** (Figure 4a and 4b), **7**, or **8** (data not shown) does not instigate translocation. These ligands,

which were the least effective at displacing ^{3}H-Mibolerone in the receptor binding assay (Table 1),[15] are also not capable of inhibiting the action of 1.0 nM Mibolerone on AR-GFP (Figure 4c and 4d). Of interest is the result obtained from treatment of the cells with **4**. While this compound was not able to instigate translocation of AR-GFP at concentrations up to 1.0 μM (Figure 4e and 4f), it did serve to partially inhibit the activity of 1.0 nM Mibolerone on treated cells (Figure 4g and 4h).

The most encouraging results obtained for any of the tested compounds came from **6a** (Figure 4i and 4j). Treatment of AR-GFP-expressing cells with the butyne-tethered product at a concentration of 1.0 μM successfully caused nuclear localization of the receptor. Although the binding efficiency of the antiandrogens is not directly related to their ability to initiate translocation, we have found that, in the tested series, the compound which is most effective at competing for AR binding with ^{3}H-Mibolerone is also capable of initiating migration of the AR-GFP receptor to the nucleus. These findings qualify **6**a as a lead compound for further development as a delivery vehicle for the doxorubicin prodrug **1a**.

Following the identification of a viable targeting group, we sought to evaluate a targeted derivative **9** of the prodrug **1a** via the AR binding assay, just as the targeting groups had been evaluated. Since the AR-GFP translocation assay must be run at 37 °C, and the N-Mannich base **9** readily hydrolyzes to regenerate **6a**, the *O*-butyryloxymethylene-protected **10** was prepared for use as a stable derivative. We have found that acyloxymethylation of the phenolic moiety of salicylamide leads to a stable N-Mannich base product upon reaction with doxorubicin.[5] Preparation of this derivative allows for study of the intact prodrug without concern for the activity of **6a**, which is released upon partial hydrolysis of **9** and can be expected to compete for AR binding. Competitive binding of both **9** and **10** has been confirmed using the cell free assay. Both compounds demonstrate binding affinities similar to that of **6a** (Table 1), and both have been shown to be stable under the assay conditions (30 min incubation at 4 °C).[15]

Treatment of AR-GFP-expressing PC3 cells with 1.0 μM **10** indicated that, unlike **6a**, the full prodrug **10** did not instigate translocation into the nucleus (Figure 4 k and 4l). However, the presence of 1.0 μM **10** did serve to inhibit the action of 1.0 nM Mibolerone on the AR-GFP receptor (Figure 4m and 4n). The exact cause for the loss of activity upon introduction of the doxorubicin N-Mannich base is not clear. It is possible that the tether portion of the targeting group is too short, allowing for interactions between doxorubicin and the receptor, which serve to preclude the necessary conformational change of the AR. We have also explored the possibility that the introduction of the butyryloxymethylene protecting group to **6a** is responsible for the loss of activity. This construct **6b**, however, was found to act in much the same manner as **6a**, causing nuclear translocation of the AR upon binding (data not shown). Unfortunately, the assay cannot be used to evaluate the unprotected construct **9**, because of the inherent instability of the prodrug. It should be noted, however, that comparison of Figure 4n with Figure 4d shows a clear distinction between the activity of an efficient AR binder like **10** and a lower affinity ligand such as **5**. Compound **10** inhibits the action of Mibolerone, while **5** does not.

The targeted prodrug **9** was also evaluated in cytotoxicity experiments employing the androgen receptor-expressing PC3/AR and control PC3/neo cell lines. PC3/AR and PC3/neo cells, provided by Dr. Kerry L. Burnstein, University of Miami, Miami, FL, were treated for 3, 10, and 20 min with either 500 nM doxorubicin or 500 nM **9**. The short dosing periods were chosen to capitalize on any binding of the prodrug to the AR which would serve to concentrate it in the cells. Earlier experiments employing a 4 h treatment had shown no difference in effect between the targeted prodrug and doxorubicin due to the constant exposure of the cells to cytotoxin released from hydrolysis of the N-Mannich base.[15] We hypothesized that rapid removal of doxorubicin would leave little drug in the cells, while binding of **9** to the AR would serve to retain the prodrug after removal of the treatment solution. No difference was observed, however, at any treatment time. Several factors may account for this, including relatively poor or excessively slow binding, insufficient cytotoxicity of doxorubicin, or equally extensive uptake of both the targeted and untargeted drug by cultured cells, independent of AR binding. To address the shortcomings of our construct in cultured cells, we have also investigated the cellular distribution of doxorubicin, doxsaliform, and the targeted prodrug **10**.

The fluorescence of doxorubicin can be monitored in order to determine the rate of uptake and intracellular distribution of the anthraquinone fluorophore. Curiously, the fluorescence of doxorubicin is partially quenched by the introduction of salicylamide in the N-Mannich base construct as in **1a** and **9**. However, modification of the phenolic moiety of salicylamide with the butyryloxymethylene protecting group serves to fully restore fluorescence in **10**. These interesting observations allow for the tracking of both the targeted prodrug **10**, as well as the intracellular distribution of doxorubicin, which fluoresces, once it is released from **9** in which fluorescence is greatly attenuated.

The *O*-acetyloxymethylene derivative of doxsaliform **1b** (Figure 1) was prepared to allow for comparison of the targeted and untargeted prodrugs.[5] The initial distribution of **10** was predominantly cytosolic, with noticeable accumulation in several focal points throughout both PC3/AR (Figure 5a) and PC3/neo (Figure 5b) cells. Similar localization was observed for **1b** upon initial treatment with a 500 nM solution of the prodrug (not shown). However, fluorescence from **1b** was seen to accumulate, at least to some extent over time (> 3 h), in the nuclei and in some perinuclear depots of treated cells (Figure 5c). The origin of this nuclear fluorescence is yet uncertain since any hydrolysis of **1b** (which is perhaps dependent on any intracellular esterase activity) releases doxorubicin, which shows its own pattern of distribution. Faint fluorescence in the nuclei of cells treated with **1b** may be due to limited accumulation of **1b** or complete accumulation of small amounts of liberated doxorubicin, which is seen to rapidly localize to the nucleus (Figure 5d). It should be noted that similar 3 h treatment of the same cell lines with **1a**, in which hydrolysis of the N-Mannich base is

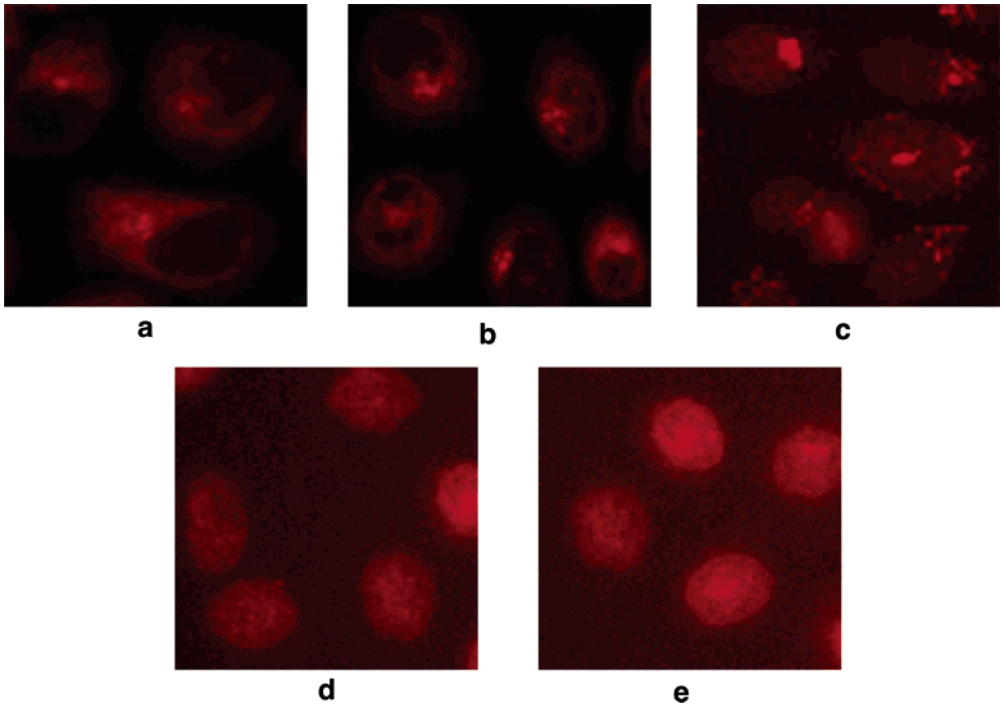

Figure 5. Fluorescence at 590 nm from doxorubicin fluorophore in (a) PC3/AR cells 20 min after treatment with 500 nM **10**; (b) PC3/neo cells 20 min after treatment with 500 nM **10**; (c) localization of fluorescence after 210 min treatment of PC3/AR cells with 500 nM **1b**; (d) nuclear localization of doxorubicin hydrochloride in PC3/AR cells treated with 2 μM drug solution for 40 min; (e) nuclear localization of doxorubicin in PC3/AR cells 3.5 h after treatment with 500 nM **9**.

not retarded, leads to exclusive nuclear accumulation of fluorescence (data not shown). Since the half-life of hydrolysis for **1a** is approximately 57 min, this nuclear fluorescnce at 3 h is attributed entirely to liberated doxorubicin.[5]

The variable intensity of fluorescence observed due to accumulation of free doxorubicin or the various prodrugs, as well as the inherent instability of the N-Mannich bases, makes continuous tracking of these constructs over time a difficult task. What is more useful is the comparison of the deposition of the targeted prodrugs **9** and **10** with the deposition of doxorubicin upon initial dosing and after sufficient time for release of the N-Mannich base trigger. Figure 5e shows the primarily nuclear localization of fluorescence resulting after 3 h treatment with the active targeted prodrug **9**. The fluorescence is attributed to doxorubicin, which accumulates after hydrolysis of the prodrug over the 3 h treatment time. These results together with those obtained from following the fluorescence of **10**, which remains primarily cytosolic over time, suggest that the prodrug **9** releases doxorubicin in the cytosol of treated cells and not in the nucleus. In addition, the similar distribution of fluorescence observed in both AR-expressing PC3/AR and nonexpressing PC3/neo cells (Figure 5a and 5b, respectively) indicates that the bulk of the prodrug retained by the cells is not associated with the AR. This further supports the proposal that measurements of cytotoxicity in cell culture are not sufficient to determine the targeting ability of **9**, since the prodrug readily accumulates in treated cells, regardless of AR content. Whether in vivo targeting of the prodrug can overcome this non-AR specific accumulation is yet to be determined.

Conclusions

We have demonstrated that nonsteroidal antiandrogens modified with an appropriate tether retain reasonable binding affinity for the AR and initiate nuclear translocation of the receptor. We have further shown that a prodrug of doxorubicin can be successfully targeted to cells via specific interaction with the AR. Despite these results, several shortcomings of the lead molecules identified herein need to be addressed. No improvement in cytotoxicity was observed, relative to doxorubicin, upon treatment of PC3/AR and PC3/neo cells with the targeted prodrug **9**. While this result is less than encouraging, it does not necessarily indicate that the targeting of the AR is insufficient as a means of delivering active cytotoxin to cancerous cells.

Previous work in our laboratory has shown that treatment of doxorubicin sensitive or resistant cells with doxoform, a simple prodrug of doxorubicin−formaldehyde conjugate (Figure 2), leads to greatly superior cell killing relative to doxorubicin alone or in the presence of free formaldehyde.[1] In unpublished data, we have observed the accumulation of fluorescent drug in a perinuclear space, possibly the Golgi apparatus, after treatment of cultured cells with doxoform. This is in sharp contrast to the accumulation of drug in the nucleus that is observed upon treatment with unmodified doxorubicin. These apparently paradoxical results would suggest that the ultimate site of action of the anthracycline is, in fact, not the nucleus. While this possibility cannot be ruled out, there are several factors that cloud the issue. Fluorescence microscopy has proven to be somewhat ambiguous as a means of determining where anthracyclines accumulate in cells. The fluorescence of doxorubicin is quenched by DNA intercalation[32,33] and enhanced by association with

lipids.[34] Also, while doxoform appears to target a perinuclear region in live cells, it is found to be primarily nuclear in cells that are fixed with methanol after drug treatment.[9] These facts greatly hinder the quantification of drug within various cellular compartments. Furthermore, while any intercalated drug may not be visible due to quenching, the appearance of exclusive perinuclear fluorescence in live cells treated with doxoform may be attributed to enhanced fluorescence of drug associated with the Golgi apparatus or other lipid membranes. It is likely that the fixing process releases drug from one or more sites of intracellular deposition, which may include nuclear DNA, in which fluorescence of the drug is initially quenched.[35] This would explain the different distribution of fluorescence in live and fixed cells treated with doxoform. Likewise, the fluorescence of doxorubicin in the nuclei of treated cells, either delivered as the parent drug or released from an N-Mannich base construct, may be attributed to association with the nuclear membrane (fluorescence enhancing) and not necessarily DNA (fluorescence quenching). At this point, we must consider the possibility that a small number of fluorometrically undetectable DNA−drug adducts, resulting from formaldehyde released by the dimeric prodrug, are responsible for the superior cytotoxicity of doxoform. It is also possible that the ultimate site of action of doxoform is somewhere other than nuclear DNA. What we can conclude here is that the localization of doxorubicin−formaldehyde conjugates to the cytosol via AR targeting offers no improvement in cytotoxicity relative to the untargeted drug.

Since there is a great disparity between the activities of doxoform and conjugates which accumulate in the cytosol, such as the N-Mannich base **9**, it would appear that delivery of the prodrug to the appropriate locus is critical for reaping the benefits of coadministered formaldehyde. To this end, future work will focus on lead optimization through the modification of the butyne tether of **6a**. While incorporation of a triple bond in the tether has been shown to be critical for nuclear migration in the translocation assay, addition of the doxorubicin N-Mannich base serves to abolish this activity. Homologous tethers that vary in length and, perhaps, functionality, may reinstate the nuclear accumulation of the AR bound ligand. By accomplishing this, we may be able to determine not only if delivery of the N-Mannich base to the nucleus is sufficient to increase the cytotoxicity of doxorubicin, but if nuclear DNA is, in fact, the ultimate site of action of the supertoxic doxoform. Finally, despite the failure to deliver the prodrug to the nucleus, in vivo mouse studies are planned in an effort to assess whether binding of the AR is sufficient for accumulation of **9** within tumors.

Experimental Section

General Remarks. ^{1}H NMR spectra were acquired with a Varian Unity Inova 500 MHz spectrometer. Unambiguous NMR assignments for the protons of the nilutamide, salicylamide, and doxorubicin portions of 10 are designated by "nil", "sal", or "dox" respectively. Mass spectral data were acquired on a VG Instruments AutospecM mass spectrometer by liquid SIMS (LSIMS) ionization with a poly(ethylene glycol) (PEG) internal standard for [MH^+] data. Mass spectral data [MNa^+] for compound **10** were collected by Dr. Chris Hadad (Ohio State University; Columbus, OH) with a 3-Tesla Finnigan FTMS-2000 Fourier Transform mass spectrometer. UV−vis spectrometry was performed with a Hewlett-Packard 8452A diode array spectrophotometer and workstation. Fluorescence microscopy was conducted with a Leica DM IRB stereo microscope equipped with an ebq 100 mercury lamp power source. Fluorescence of doxorubicin and derivatives was monitored at wavelengths above 590 nm, with excitation at 540 ± 20 nm. DAPI fluorescence was observed at wavelengths above 425 nm with excitation at 360 ± 20 nm. Green fluorescent protein was observed at wavelengths above 515 nm with excitation at 470 ± 20 nm. HPLC analyses were performed with a Hewlett-Packard 1090 liquid chromatograph equipped with a diode array UV−vis detector and workstation; chromatography was performed with a Hewlett-Packard 5 μm reverse phase C_{18} microbore column, 2.1 mm i.d. × 100 mm, eluting at 0.5 mL/min, monitoring at 260, 310, and 480 nm. Acceptable analytical resolution was achieved with gradients of acetonitrile and triethylammonium acetate (Et_3NHOAc; TEAA), prepared as 20 mM triethylamine adjusted to pH 6.0 with acetic acid. The method employed for all analytical chromatography was as follows: A = CH_3CN, B = pH 6.0 buffer; A:B, 0:100 to 70:30 at 10 min, isocratic until 12 min, 0:100 at 15 min. For preparative HPLC, a 5 μm spherical particle C_{18} Ranin Dynamax semipreparative column was employed, 10 mm × 25 cm with a 10 mm × 5 cm guard column, eluting at 3.0 mL/min, monitoring at 260, 310, and 480 nm. Adequate preparative separation was achieved using the following method: A = CH_3CN, B = 1% aqueous HCl; A:B, 50:50 to 55:45 at 20 min, isocratic until 25 min, 70:30 at 30 min, isocratic until 35 min, 50:50 at 40 min. Water was distilled and purified with a Millipore Q-UF Plus purification system to 18 Mohm-cm. Flash silica gel (particle size: 32−63 μm, pore size: 60 Å, Cat# 02826−25) was obtained from Scientific Adsorbants Inc. (Atlanta, GA). Formalin (37% w/w formaldehyde in water/methanol), triethylamine (99%), magnesium sulfate (anhydrous; 99.8%), sodium chloride (99.9%), HPLC grade acetonitrile, potassium iodide (ACS), and potassium carbonate (anhydrous; 99.8%) were purchased from Fisher (Fair Lawn, NJ). Acetic acid was purchased from Mallinckrodt (Paris, KY). Sure Seal anhydrous *N*,*N*-dimethylformamide (99.8%) was purchsed from Aldrich (Milwaukee, WI). Doxorubicin hydrochloride (99%) was obtained from Hande Tech Development Co. (Houston, TX). Chloromethyl butyrate (98%) was purchased from Acros Organics (Pittsburgh, PA). FUGENE 6 transfection reagent and the Complete-mini protease inhibitor cocktail were obtained from Roche (Basel, Switzerland). The syntheses of compounds **1b**, **4**, **5**, **6a**, **7**, **8**, and **9** have been previously reported, as have the methodologies employed in the competitive binding and IC50 measurements of compounds **9** and **10**.[5,15]

All tissue culture materials were obtained from Gibco Life Technologies (Grand Island, NY) unless otherwise noted. PC3/AR and PC3/neo cells were a gift from Dr. Kerry L. Burnstein (University of Miami, FL). The pEGFP-C2 rcAR plasmid was a gift from Dr. Arun Roy (UTHSC; San Antonio, TX). All cell lines were maintained in vitro by serial culture in RPMI 1640 media supplemented with either 10% fetal bovine serum (Gemini Bio-Products, Calbasas, CA) or dextran−charcoal-stripped (delipidated) fetal calf serum (Sigma, Milwaukee, WI) as indicated, l-glutamine (2 mM), HEPES buffer (10 mM), penicillin (100 units/mL), and streptomycin (100 μg/mL). Cells were maintained at 37 °C in a humidified atmosphere of 5% CO_2 and 95% air. Phenol red-free RPMI 1640 media supplemented with L-glutamine was obtained from Sigma (Milwaukee, WI).

Syntheses. 5-{4-[3-(4-Cyano-3-trifluoromethyl-phenyl)-5,5-dimethyl-2,4-dioxo-imidazolidin-1yl]-but-2-ynyloxymethyl}-2-butyryloxymethoxy-benzamide (6b). The procedure was based upon that reported by Bundgaard for the synthesis of 2-butyryloxymethoxybenzamide.[36] A mixture of 40 mg (0.078 mmol) of **6a** and 21 mg (0.15 mmol) of potassium carbonate was stirred for 30 min at room temperature in 5 mL of acetone. In a separate flask, 16 mg (0.12 mmol) of chloromethyl butyrate and 22 mg (0.13 mmol) of potassium

iodide were stirred in 5 mL of acetone at room temperature. The two mixtures were then combined and refluxed for 4 h. The reaction was stopped by cooling to room temperature and filtering through a glass frit. The collected liquid was rotary evaporated at 30 °C, and the residue was dissolved in 100 mL of ethyl acetate. After 3× washes with 50 mL of saturated brine, the organic layer was collected, dried over anhydrous magnesium sulfate, and concentrated by rotary evaporation at 40 °C. The washed product was then dissolved in 3 mL of ethyl acetate and introduced to a silica gel flash column (2 cm × 30 cm) packed in 50% hexanes/50% ethyl acetate. The desired product was eluted with 25% hexanes/75% ethyl acetate. Concentration by rotary evaporation at 30 °C yielded approximately 80% conversion. The semipure product was characterized by the following spectral properties and was used without further purification for the preparation of **10**; ^{1}H NMR (500 MHz, $CDCl_3$) δ 0.95 (3H, t, J = 7 Hz, Bu-4), 1.63−1.71 (2H, m, Bu-3), 1.67 (6H, s, 5-CH_3's), 2.37 (2H, t, J = 8 Hz, Bu-2), 4.20 (2H, s, tether-3), 4.34 (2H, s, tether-6), 4.59 (2H, s, tether-1), 5.91 (2H, s, OCH_2O), 6.06 (1H, bs, NH), 7.18 (1H, d, J = 8 Hz, 3), 7.52 (1H, dd, J = 8, 2 Hz, 4), 7.57 (1H, bs, NH), 7.95 (1H, d, J = 8 Hz, 5), 8.03 (1H, dd, J = 8, 2 Hz, 6), 8.18 (2H, s, 6/2); mass spectrum, *m/z* 615.2064 [MH^+] (calculated for 615.2067).

***N*-(5-{4-[3-(4-Cyano-3-trifluoromethyl-phenyl)-5,5-dimethyl-2,4-dioxo-imidazolidin-1-yl]-but-2-ynyloxymethyl}-2-butyryloxymethoxybenzamidomethyl)-doxorubicin (10).** To a stirring solution of 20 mg of **6b** (0.033 mmol) in 2.0 mL of DMF was added 10 μL of a 37% formalin solution (0.13 mmol). The reaction was stirred in a screw top vial for 15 min at 55 °C, at which time 20 mg (0.034 mmol) of doxorubicin hydrochloride was added to form a red suspension which was stirred at 55 °C. After 15 min, a clear red solution had formed and the reaction was removed from the heat. Transfer of the solution to a 250 mL round-bottom flask, followed by rotary evaporation at 55 °C and 50 μmHg gave a red film which was readily dissolved in 20 mL of methanol containing 30% of 20 mM pH 2.9 1% TFA. After 10 min at room temperature, the methanol was removed by rotary evaporation at 30 °C and the resulting aqueous suspension was diluted to 100 mL with saturated brine and transferred to a separatory funnel. Extraction into 50 mL of chloroform followed by rotary evaporation at 30 °C gave a red film. The product was then dissolved in 1−2 mL of methanol and filtered through a 0.45 μm Spin-X centrifuge filter. Purification was achieved by preparative HPLC using a pH 3.5 TEAA buffer as the aqueous eluent. Pure material was collected into a test tube (100 mm × 10 mm) containing 0.5 mL of 1.0 M HCl. Acetonitrile was removed by rotary evaporation at 30 °C to yield an aqueous suspension of the pure product which was diluted to 50 mL with saturated brine and transferred to a separatory funnel. Extraction into 50 mL of chloroform followed by rotary evaporation at 30 °C gave 30 mg (76%) of **10** as the free base; ^{1}H NMR (500 MHz, ($CDCl_3$) δ 0.85 (3H, t, J = 7 Hz, $OOCCH_2CH_2CH_3$), 1.40 (3H, d, J = 7 Hz, dox-5′-CH_3), 1.49−1.61 (2H, m, $OOCCH_2CH_2CH_3$), 1.60−1.68 (1H, m, dox-2′), 1.63 (6H, s, nil-5-$(CH_3)_2$), 1.84 (1H, td, J = 13, 4 Hz, dox-2′), 2.15 (1H, dd, J = 4, 15 Hz, dox-8), 2.20−2.30 (2H, m, $OOCCH_2CH_2CH_3$), 2.33−2.39 (1H, dt, J = 15, 2 Hz, dox-8), 3.03 (1H, bs, dox-14-OH), 3.04 (1H, d, J = 19 Hz, dox-10), 3.06−3.13 (1H, bm, dox-3′), 3.22 (1H, dd, J = 2, 19 Hz, dox-10), 3.75 (1H, bs, dox-4′), 4.02 (1H, q, J = 6 Hz, dox-5′), 4.09 (3H, s, dox-4-OCH_3), 4.15 (2H, t, J = 2 Hz, CCH_2NCO), 4.30 (2H, t, J = 2 Hz, $BnOCH_2C$), 4.35 (2H, d, J = 6 Hz, NCH_2N), 4.51 (2H, s, Bn CH_2), 4.67 (1H, d, J = 21 Hz, 14), 4.69 (1H, d, J = 21 Hz, 14), 4.81 (1H, s, 9-OH), 5.35 (1H, m, dox-7), 5.56 (1H, d, J = 4 Hz, dox-1′), 5.68 (1H, d, J = 7 Hz, OCH_2O), 5.78 (1H, d, J = 7 Hz, OCH_2O), 7.08 (1H, d, J = 8 Hz, sal-3), 7.41 (1H, dd, J = 1, 8 Hz, dox-3), 7.42 (1H, dd, J = 2, 8 Hz, sal-4), 7.80 (1H, t, J = 8 Hz, dox-2), 7.93 (1H, d, J = 9 Hz, nil-5), 8.01 (1H, dd, J = 2, 9 Hz, nil-6), 8.03 (1H, dd, J = 1, 8 Hz, dox-1), 8.05 (1H, d, J = 2, sal-6), 8.15 (1H, d, J = 2 Hz, nil-2), 7.96−8.06 (1H, bm, NH), 13.27 (1H, s, dox-6/11-OH), 13.97 (1H, s, dox-6/11-OH); mass spectrum, *m/z* 1192.3665 [MNa^+] (calculated for 1192.3621).

AR-GFP Localization by Fluorescence Microscopy. PC3 cells were dissociated with trypsin EDTA, counted, and suspended in growth media to a concentration of 3.5 × 10^4 cells/mL. This cell suspension was dispensed in 2 mL aliquots into six-well tissue culture plates. Plates were then incubated for 12 h at 37 °C in a humidified atmosphere of 5% CO_2 and 95% air. A transfection cocktail was prepared by adding 8 μL of FUGENE 6 transfection reagent to sterile sample tubes containing 100 μL of serum free, phenol red-free RPMI 1640 medium for each well to be transfected. To each solution was added 2 μL of a 800 μg/mL solution of the pEGFP-C2 rcAR plasmid in Millipore water. After gentle mixing, the transfection cocktail was allowed to incubate at room temperature for 40 min. At this time, 100 μL of transfection cocktail was added to each well of 12 h old cells. The cells were then incubated for 24 h at 37 °C in a humidified atmosphere of 5% CO_2 and 95% air. The transfection medium was then removed and the cells were washed with 1 mL of FBS free, phenol red-free RPMI 1640 growth medium. Following the wash, 1 mL of phenol red-free RPMI 1640 medium supplemented with dextran-coated charcoal-stripped FBS was added to each well, and the cells were incubated for an additional 24 h. The growth medium was again replaced with 1 mL of phenol red-free RPMI supplemented with dextran-coated charcoal-stripped FBS. Candidate AR-GFP-expressing cells in each well were identified and marked before appropriate concentrations of the test compounds were added in 10 μL of sterile DMSO. The treated cells were then incubated for the necessary time at 37 °C before marked AR-GFP-expressing cells were observed for drug activity. Nuclear staining with DAPI was carried out by 15 min treatment with 1 mL of a 1% gluteraldahyde solution, followed by 15 min treatment with 1 mL of 0.2 μg/mL DAPI in phenol red-free RPMI 1640. The DAPI solution was then replaced with 1 mL of phenol red-free RPMI 1640 and fluorescence over 425 nm was observed at 400× with excitation at 360 ± 20 nm.

Doxorubicin Localization by Fluorescence Microscopy. Cells were dissociated with trypsin EDTA, counted, and suspended in growth media to a concentration of 3.5 × 10^4 cells/mL. This cell suspension was dispensed in 2 mL aliquots into six-well tissue culture plates. Plates were then incubated for 36 h at 37 °C in a humidified atmosphere of 5% CO_2 and 95% air. The medium was replaced with 1 mL of phenol red-free RPMI 1640 growth medium supplemented with 10% dextran-coated charcoal-stripped FBS prior to addition of the test compound. The appropriate compound was dissolved in DMSO, and the concentration was adjusted to 50−200 μM by measuring the solution absorbance at 480 nm. Addition of 10 μL of the appropriate doxorubicin or prodrug solution was followed by incubation at 37 °C as indicated. The drug solution in individual wells was removed at the appropriate time, and the cells were washed with 1 mL of the phenol red-free growth medium. The washed cells were then supplemented with 1 mL of phenol-red free growth medium for imaging.

Radioligand Competition AR Binding Assay. PC3/AR or PC3/neo cells were grown in RPMI 1640 medium to approximately 80% confluency in five Nunc T-175 flasks. Growth medium in each flask was then replaced with 50 mL of phenol red-free RPMI 1640 supplemented with 10% dextran-coated charcoal-stripped FBS, and the cells were grown for an additional 18−22 h. Two hours prior to harvesting, the growth medium was again replaced with fresh phenol red-free, charcoal-stripped RPMI. The cells were then washed with 10 mL of Hank's balanced salt solution and dissociated with trypsin. Trypsin was quenched with phenol red-free, charcoal-stripped RPMI, and the combined cells from each flask were centrifuged in a 50 mL conical tube at 100*g* for 5 min. The cells were then resuspended in 50 mL of phenol red-free, charcoal-stripped RPMI and counted at this concentration. Centrifugation at 100*g* gave approximately 1 mL of cells which were resuspended in 5 mL of 4 °C lysis buffer (10 mM Tris, 1.5 mM EDTA, 0.5 mM DTT, 10 mM $NaMoO_4$, 1.0 mM PMSF, 10% v/v glycerol) supplemented immediately before use with Complete-mini protease inhibitor cocktail. Cells were lysed via

sonication at 4 °C with a microtip, set at maximum power, for 10 cycles of 6 s on and 24 s off. The cytosolic fraction of the lysate was isolated by ultracentrifugation at 4 °C and 225 000*g* for 45 min. The centrifuged samples were dispensed into 100 μL aliquots and stored at −78 °C until used. Total protein was quantified either in fresh or frozen aliquots by the Sigma BSA micro protein determination method according to the prescribed protocol.

Aliquots of cell lysate were used fresh or thawed at 4 °C. Stock solutions of 100× working concentration of the test ligands, ^{3}H-Mibolerone and unlabled Mibolerone were prepared in DMSO and subsequently diluted to 10× in lysis buffer. Concentrations of test compounds were determined spectrophotometricly in DMSO by either absorbance at 310 nm for salicylamide containing molecules (ϵ_{310} = 3580 L/(mol × cm); as determined from a Beer−Lambert plot described by varying concentrations of salicylamide), 264 nm for **2b** (ϵ_{264} = 13 000 L/(mol × cm)), or 276 nm for **2a** (ϵ_{276} = 4620 L/(mol × cm)). Aliquots of cell lysate were complemented with 10 μL of 10× ligand solutions and 10 μL of the 10× ^{3}H-Mibolerone solution to yield concentrations of 1, 10, 100, and 1000 nM test compound and 1 nM ^{3}H-Mibolerone. Each reaction was prepared in duplicate to yield eight total test assays. Duplicate positive controls, consisting of 10 μL of lysis buffer in place of a test ligand (total radioligand binding), and negative controls, consisting of 1000 nM unlabled Mibolerone (nonspecific binding), each in the presence of 1 nM ^{3}H-Mibolerone, were prepared. The reactions were gently mixed and briefly centrifuged before incubating at 4 °C for 30 min. After incubation was complete, 100 μL of each reaction was introduced to 400 μL of ice cold hydroxyapatite (HA), as a 60% suspension in pH 7.4 Tris buffer, on a 0.45 μm nylon filter in a Spin-X centrifuge tube. Upon addition of the reaction solution, the tubes were closed, briefly vortexed, and allowed to incubate on ice for 12 min with vortexing every 3−5 min. The HA suspensions were then centrifuged at 1200*g* for 10 min. The filtrate was discarded and the dry pellet was resuspended in 400 μL of pH 7.3 20 mM Tris wash buffer containing 0.1% Triton-X100. Following seven rounds of resuspension and subsequent centrifugation, the final filtrate was discarded and the dry pellet was centrifuged for an additional 15 min. The pellet and filter bucket for each sample were then transferred to 20 mL scintillation vials and 4 mL of scintillation cocktail was added to each. Vortexing for 30 s thoroughly mixed the pellet with the scintillation liquid before counting. Each sample was counted for 5 repetitions of 3 min counts. This counting protocol was then repeated two additional times to ensure precision. Specific binding for each test concentration was determined by subtracting the nonspecific binding control from the total binding determined for each concentration. Comparison to the specific binding for the positive control, in which no competing ligand was incubated with the ^{3}H-Mibolerone, yielded the percent of ^{3}H-Mibolerone displaced by a given concentration of test ligand. The IC_{50} values for each test ligand were calculated by Logit-log(pseudo-Hill) analysis.

Cytotoxicity. In an attempt to determine targeting of **9** in PC3/AR and PC3/neo cells, cells were dissociated with trypsin EDTA, counted, and suspended in fully supplemented growth media to a concentration of 2.5 × 10^3 cells/mL. This cell suspension was dispensed in 200 μL aliquots into 96-well plates and was incubated for 36 h at 37 °C in a humidifed atmosphere of 5% CO_2 and 95% air. After 36 h growth, the medium was replaced with 180 μL phenol red-free RPMI 1640 supplemented with 10% dextran-coated charcoal-stripped FBS, and the cells were allowed to grow an additional 24 h. Solutions of **9** and doxorubicin were prepared in DMSO at a 100× working concentration of 50 μM as determined by the 480 nm absorbance of the solution. After sterile filtration, the DMSO solutions were diluted 1:10 in phenol red-free, charcoal-stripped RPMI medium; 20 μL of the appropriate 10× drug solution was immediately added to three lanes of both PC3/AR and PC3/neo cells. Additionally, two lanes were treated with 20 μL of stripped medium containing 10% DMSO, and one lane was treated with 200 μL of 1.5 M Tris in Millipore water. After 5, 10, and 20 min, the drug solution was removed from one lane of treated cells and replaced with 100 μL of phenol red-free, charcoal-stripped RPMI medium. Media in the control lanes was replaced after 20 min. The cells were incubated for 12 h at 37 °C, at which time 200 μL of fully supplemented RPMI 1640 growth medium was added to each well, *without* removal of the stripped medium. Cells were allowed to grow for 6 days at 37 °C in a humidified atmosphere of 5% CO_2 and 95% air.

The extent of colony formation was determined by use of a crystal violet staining assay. Cells were fixed with 200 μL of 1% gluteraldehyde in Hank's balanced salt solution. The cells were then stained with 100 μL of 0.1% crystal violet in Millipore water for 30 min. Following removal of the crystal violet solution, plates were submerged in distilled water and shaken vigorously to remove the excess water. After several hours drying time, 200 μL of 70% ethanol was added to each well to solubilize the dye. The plates were stored at 4 °C for 4 h as the dye was extracted from the cells. The optical density of each well was then measured on an ELISA plate reader at 588 nm. Relative colony size was established by comparison of the drug-treated lanes to the control lanes.

Acknowledgment. We thank Dr. Arun Roy (UTHSC, San Antonio, TX) for the plasmid containing the AR-GFP construct and Dr. Kerry L. Burnstein (University of Miami, Miami, Fl) for PC3/AR and PC3/neo cells. We are grateful to the U.S. Army Prostate Cancer Research Program (DAMD17-01-1-0046) and the National Cancer Institute of the NIH (CA-92107) for financial support and the National Science Foundation for help with the purchase of NMR equipment (CHE-0131003). T.H.K. thanks the University of Colorado Council for Research and Creative Work for a Faculty Fellowship.

Supporting Information Available: HPLC chromatogram, to confirm purity of compound **10,** and ^{1}H NMR spectra for compounds **6b** and **10**. This material is available free of charge via the Internet at http://pubs.acs.org.

References

(1) Fenick, D. J.; Taatjes, D. J.; Koch, T. H. Doxoform and Daunoform: Anthracycline-formaldehyde conjugates toxic to resistant tumor cells. *J. Med. Chem.* **1997**, *40*, 2452−2461.
(2) Dernell, W. S.; Powers, B. E.; Taatjes, D. J.; Cogan, P.; Gaudiano, G. et al. Evaluation of the epidoxorubicin-formaldehyde conjugate, epidoxoform, in a mouse mammary carcinoma model. *Cancer Invest.* **2002**, *20*, 712−723.
(3) Cutts, S. M.; Rephaeli, A.; Nudelman, A.; Hmelnitsky, I.; Phillips, D. R. Molecular basis for the synergistic interaction of adriamycin with the formaldehyde-releasing prodrug pivaloyloxymethyl butyrate (AN-9). *Cancer Res.* **2001**, *61*, 8194−8202.
(4) Swift, L. P.; Cutts, S. M.; Rephaeli, A.; Nudelman, A.; Phillips, D. R. Activation of Adriamycin by the pH-dependent formaldehyde-releasing prodrug hexamethylenetetramine. *Mol. Cancer Ther.* **2003**, *2*, 189−198.
(5) Cogan, P. S.; Fowler, C. R.; Post, G. C.; Koch, T. H. Doxsaliform: a novel N-Mannich base prodrug of a doxorubicin formaldehyde conjugate. *Lett. Drug Des. Dis.* **2004**, *1*, 247−255.
(6) Taatjes, D. J.; Fenick, D. J.; Koch, T. H. Epidoxoform: a hydrolytically more stable anthracycline-formaldehyde conjugate, cytotoxic to resistant tumor cells. *J. Med. Chem.* **1998**, *41*, 1306−1314.
(7) Zeman, S. M.; Phillips, D. R.; Crothers, D. M. Characterization of covalent Adriamycin-DNA adducts. *Proc. Natl. Acad. Sci. U.S.A.* **1998**, *95*, 11561−11565.
(8) Podell, E. R.; Harrington, D. J.; Taatjes, D. J.; Koch, T. H. Crystal structure of epidoxorubicin-formaldehyde virtual cross-link of DNA and evidence for its formation in human breast-cancer cells. *Acta Crystallogr.* **1999**, *D55*, 1516−1523.
(9) Taatjes, D. J.; Fenick, D. J.; Koch, T. H. Nuclear targeting and nuclear retention of anthracycline-formaldehyde conjugates implicates DNA covalent bonding in the cytotoxic mechanism of anthracyclines. *Chem. Res. Toxicol.* **1999**, *12*, 588−596.
(10) Cullinane, C.; Cutts, S. M.; Panousis, C.; Phillips, D. R. Interstrand cross-linking by Adriamycin in nuclear and mitochondrial DNA of MCF-7 cells. *Nucleic Acid. Res.* **2000**, *28*, 1019−1025.

(11) Anderson, W. F.; Chatterjee, N.; Ershler, W. B.; Brawley, O. W. Estrogen receptor breast cancer phenotypes in surveillance, epidemiology, and end results databases. *Breast Cancer Res. Tr.* **2002**, *76*, 27−36.
(12) Burke, P. J.; Koch, T. H. Design, synthesis, and biological evaluation of doxorubicin−formaldehyde conjugates targeted to breast cancer cells. *J. Med. Chem.* **2004**, *47*, 1193−1206.
(13) Zitzmann, S.; Ehemann, V.; Schwab, M. Arginine-glycine-aspartic acid (RGD)-peptide binds to both tumor and tumor-endothelial cells *in vivo*. *Cancer Res.* **2002**, *62*, 5139−5143.
(14) Arap, W.; Oasqualini, R.; Ruoslahti, E. Cancer treatment by targeted drug delivery to tumor vasculature in a mouse model. *Science* **1998**, *279*, 377−380.
(15) Cogan, P. S.; Koch, T. H. Rational design and synthesis of androgen receptor-targeted nonsteroidal anti-androgen ligands for the tumor specific delivery of a doxorubicin−formaldehyde conjugate. *J. Med. Chem.* **2003**, *46*, 5258−5270.
(16) Ruizeveld de Winter, J. A.; Trapman, J.; Vermey, M.; Mulder, E.; Zegers, N. et al. Androgen receptor expression in human tissues: an immunohistochemical study. *J. Histochem. Cytochem.* **1991**, *39*, 927−936.
(17) Brys, M. Androgens and androgen receptor: do they play a role in breast cancer? *Med. Sci. Monit.* **2000**, *6*, 433−438.
(18) Hall, R.; Clements, J.; Birrell, S.; Tilley, W. Prostate-specific antigen and gross cystic disease fluid protein-15 are coexpressed in androgen receptor-positive breast tumors. *Br. J. Cancer.* **1998**, *78*, 360−365.
(19) Engehausen, D. G.; Tong, X.; Oehler, M. K.; Freund, C. T.; Schrott, K. M. et al. Androgen receptor gene mutations do not occur in ovarian cancer. *Anticancer Res.* **2000**, *20*, 815−819.
(20) Tihan, T.; Harmon, J. W.; Wan, X.; Younes, Z.; Nass, P. et al. Evidience of androgen receptor expression in squamous and adenocarcinoma of the esophagus. *Anticancer Res.* **2001**, *21*, 3107−3114.
(21) Kaiser, U.; Hofmann, J.; Schilli, M.; Wegmann, B.; Klotz, U. et al. Steroid-hormone receptors in cell lines and tumor biopsies of human lung cancer. *Int. J. Cancer.* **1996**, *67*, 357−364.
(22) Adiga, S. K.; Andritsch, I.; Rao, R. V.; Krishan, A. Androgen receptor expression and DNA content of paraffin-Embedded archival human prostate tumors. *Cytometry.* **2002**, *50*, 25−30.
(23) Shi, X.; Ma, A.; Xia, L.; Kung, H.; de ver White, R. W. Functional analysis of 44 mutant androgen receptors from human prostate cancer. *Cancer Res.* **2002**, *62*, 1496−1502.
(24) Georget, V.; Lobaccaro, J. M.; Terouanne, B.; Mangeat, p.; Nicolas, J. et al. Trafficking of the androgen receptor in living cells with fused green fluorescent protein-androgen receptor. *Mol. Cell Endocrinol.* **1997**, *129*, 17−26.
(25) Veldscholte, J.; A., B. C.; Brinkman, A. O.; Grootegoed, A.; Mulder, E. Anti-androgens and the mutated androgen receptor of LNCaP cells: differential effects on binding affinity, heat-shock protein interaction, and transcription activation. *Biochemistry* **1992**, *31*, 2393−2399.
(26) Tyagi, R. K.; Lavorvsky, Y.; Ahn, S. C.; Song, C. S.; Chatterjee, B. et al. Dynamics of intercellular movement and nucleocytoplasmic recycling of the ligand-activated androgen receptor in living cells. *Mol. Endocrinol.* **2000**, *14*, 1162−1174.
(27) Linja, M. J.; Savinainen, K. J.; Saramäki, O. R.; Tammela, T. L. J.; Vessella, R. L. et al. Amplification and overexpression of androgen receptor gene in hormone-refractory prostate cancer. *Cancer Res.* **2001**, *61*, 3550−3555.
(28) Tomura, A.; Goto, K.; Morinaga, H.; Nomura, M.; Okabe, T. et al. The subnuclear three-dimensional image analysis of androgen receptor fused to green fluorescent protein. *J. Biol. Chem.* **2001**, *276*, 28395−28401.
(29) Georget, V.; Terouanne, B.; Nicolas, J.; Sultan, C. Trafficking of the androgen receptor. *Methods Enzymol.* **1999**, *302*, 121−135.
(30) Dai, J. L.; Maiorino, C. A.; Gkonus, P. J.; Burnstein, K. L. Androgenic up-regulation of androgen receptor cDNA expression in androgen-independent prostate cancer cells. *Steroids* **1996**, *61*, 531−539.
(31) Georget, V.; Terouanne, B.; Nicolas, J.; Sultan, C. Mechanism of antiandrogen action: key role of Hsp90 in conformational change and transcriptional activity of the androgen receptor. *Biochemistry.* **2002**, *41*, 11824−11831.
(32) Crooke, S. T.; DuVernay, V. H. Fluorescence quenching of anthracyclines by subcellular fractions. *Anthracyclines Current Status and New Developments*; Academic Press: New York, 1980; pp 151−155.
(33) Roche, C. J.; Thomson, J. A.; Crothers, D. M. Site selectivity of daunomycin. *Biochemistry* **1994**, *33*, 926−935.
(34) Gallois, L.; Fiallo, M.; Laigle, A.; Priebe, W.; Garnier-Sullerot, A. The overall partitioning of anthracyclines into phosphatidyl-containing model membranes depends neither on the drug charge nor the presence of anionic phospholipids. *Eur. J. Biochem.* **1996**, *241*, 879−887.
(35) Pichon, C.; Monsigny, M.; Roche, A.-C. Intracellular localization of oligonucleotides: influence of fixative protocols. *Antisense Nucleic Acid Drug Dev.* **1999**, *9*, 89−93.
(36) Bundgaard, H.; Klixbull, U.; Falch, E. Prodrugs as drug delivery systems. 43. O-acyloxymethyl salicylamide N-Mannich bases as double prodrug forms for amines. *Int. J. Pharm.* **1986**, *29*, 19−28.

JM0495226